Research Article | Vol. 10, No. 12 / 1 December 2020 / Optical Materials Express 3051
Optical Materials EXPRESS

Giant electric field enhancement for plasmonic imaging via graphene based nanoslit optical superlens

GUANGQING DU, YU LU, NOOR UDDIN, DAYANTHA LANKANATH, XUN HOU, AND FENG CHEN*

State Key Laboratory for Manufacturing System Engineering and Shaanxi Key Laboratory of Photonics Technology for Information, School of Electronic Science and Engineering, Xi'an Jiaotong University, Xi'an, 710049, China
*chenfeng@mail.xjtu.edu.cn

Abstract: We present theoretical investigations on designing a simple double nano-slit superlens for dramatically improving imaging quality for advanced plasmonic photolithography through introducing graphene as a plasmonic integrator. It is proposed that more than 235 times enhancement of localized electric field can be assured as the graphene layer is embedded in the designed superlens. It is observed that by introducing graphene for superlensing, dominant enhancement of electric field amplitudes of interference imaging profiles can be observed at a properly designed photoresist with optimal thickness. We further show by systematically examining design parameters for the graphene-based superlens, clarifying the overall geometric and material parameter influences on the plasmonic imaging pattern characteristics. The results are attributed to the unique role of graphene participating in strong hybrid plasmonic cavity coupling modes for supporting localized electric fields of the nanoslit superlensing. This study shows proper designing of graphene-based optical superlens can potentially realize high-quality, low-cost and simple-realized nano-imaging for advanced plasmonic photolithography applications.

1. Introduction

Plasmonic superlens have attracted great attentions due to their ability to achieve patterns feature beyond the classical optical diffraction limit [1–5], which was accomplished by exploiting the plasmons confined to interface between dielectrics and metal materials. The superlens have found a variety of applications in the fields of nano-photolithography, ultra-resolution imaging, quantum well nano-technologies [6–10]. Physically, it is known that a nanoscale asperity supports localized surface plasmons for forming intensified near-field in plasmon antenna [11,12]. The tip-based superlens like nano-sphere or nano-bowtie antenna can well overcome the intrinsic bottle-neck of optical diffractive limit. Unfortunately, the low through-put capability can be usually encountered for the antenna-based surperlens due to point-to-point working fashion, which is far away from satisfying the expectation of high efficiency imaging replica. Instead, the superlens consist of nanoslit arrays milled on noble metals film can support interfering plasmonics, exhibiting huge potential for large-area fabrication of periodic nano-patterns. The plasmonic interference photolithography can well overcome the optical diffractive limit through designing cavity structured superlens, which bears intrinsic advantage of high efficiency and low cost over the conventional photolithography [13–15]. However, the plasmonic superlens for cavity interference photolithography system is frequently designed with more complex multi-layer noble film structures, usually leading the high-cost and imaging fidelity deviation due to the superlens structure errors from the designed one caused by manufacturing complexity. Especially, as for the large-scale interference photolithography, the plasmonic loss would be inevitable due

#409305 https://doi.org/10.1364/OME.409305
Journal © 2020 Received 8 Sep 2020; revised 19 Oct 2020; accepted 26 Oct 2020; published 3 Nov 2020

Optical Materials EXPRESS

to affluent electrons existing in layered metals [16,17], deteriorating the interference imaging profile contrast. Recently, graphene, a two-dimensional honeycomb lattice of carbon atoms has found great interest in exploring abundant plasmonics due to the cone-structured energy band and low loss electron system [18,19]. It is proposed that the plasmon interaction in mixed graphene-noble nanostructures can potentially give rise to electric field enhancement at tips or in between gap of designed superlens. As for noble-graphene cavity-structured superlens, much effort is being implemented to work out possible solutions using graphene to enhancing designs of simple-structured and low-cost superlens. It is highly expected that the plasmon interference imaging can be sharply amplified via initializing graphene components for improving photo-lithography pattern quality. As a result, capturing detailed components of graphene in coordination with noble structures to reconstruct a faithful replica of patterns on photoresist is crucial for designing superlens with lower plasmonic loss, and simultaneously high imaging replica ability. However, a comprehensive analysis on the imaging amplification characteristics for graphene based plasmonic superlens are not systematically so far, which is extremely important for exploring high through-put and low-cost plasmonic photolithography, enables potential developing of advanced plasmonic photolithography with high-fidelity ability.

In this paper, we theoretically investigated the electric field amplitude amplifications for plasmonic interference imaging for designed graphene based simple double nanoslits superlens. The graphene is considered as the plasmonic-sensitive medium to support the low-loss surface plasmon for the designed simple-realized sandwich structure superlens. A significant electric field enhancement of the interference image is observed from the designed superlens. Further investigations on the imaging electric field profile sensitive to the slit width, and the photoresist padding layer medium are fully carried out and optimized in details. This study enables optimal designing of graphene-based optical superlens for potentially realization of low-cost and simple-realized plasmonic nano-imaging with high-fidelity for advanced photolithography applications.

2. Results and discussion

Physically, as laser is incident on the superlens, the electron systems of silver are initially excited and then get electronically resonant state once the laser wavelength matches to the surface plasmon frequency determined by the specific designed double nanoslit-sandwich cavity geometry. Figure 1 shows the schematic of the simply designed superlens consisting of double nanoslit milled on silver film surface, in which the graphene and photoresist layers are sandwiched in the silver film slabs. Here, the noble nanoslits superlens are illuminated by incident laser in y direction. The applied laser is linearly polarized at x direction. The surface plasmons assisted by double nanoslits radiate coherently and form non-zeroth order diffractions that propagates and recorded in the photoresist (PR) layer of Ag-PR-Ag cavity of superlens. The superlens double slits have a distance as 100 nm, which is designed to satisfy the resonance laser wavelength in the current simulations. The plasmonic cavity interference within the sandwich structure of superlens plays a key role in forming periodical electric field for imaging in photoresist padding layer. The silver film slab thickness is taken as 40 nm, and the metal nanoslits width is considered as variable factor for well understanding the superlens imaging properties in these simulations. Numerically, we build a geometry of the graphene-based sandwich structured superlens, surrounded by ambient air medium. The simulations are based on Finite Element Method (FEM). A 2-D Helmholtz equation is built on the meshed geometry for describing the surface plasmon interaction processes. The Helmholtz equation is discretized at every meshes points to form a large sparse matrix. The perfect matching layers (PML) are set outside of geometrical superlens. The sandwich structured superlens, ambient air and PML zone are all divided into many small meshes. The scattering and transmitted light from the superlens structures are totally absorbed through the PML in far field. The boundary conditions at the interface between the padding layers are

Optical Materials EXPRESS

treated as continuous ones. In the current work, the low loss energy plasmonic propagation can be assured as the large-area imaging factor in this simulations. Due to the large difference between the surface and depth dimensions, it is difficult to numerically carry out the large-scale superlens imaging simulation directly. As an alternative, we have properly applied the single cell simulation instead of large area photolithography results by numerically using the periodic boundary condition. Here, 100 periodic cells are applied and each cell boxes are with 1.5 μm length. Unlike the plasmonic wavegude, in which the plasmonic mode works at multi-wavelength multiplexing mode. However, for plasmonic photolithography, the single wavelength working fashion is usually required for matching the wavelength-sensitive photoresist. We will focus on investigations of the electric field amplification and spectrum behaviour of the plasmonic hybrid mode. We obtain the numerical solutions of the Helmholtz equation via solving the built sparse matrix using FEM. The superlens can be technically fabricated via layer-by-layer procedures and electron beam lithography. The photoresist layer on the silver slab substrate can be prepared by the spinning film method, and the mono-layer graphene would be coated on the photoresist layer via Chemical Vapor Deposition (CVD) method.

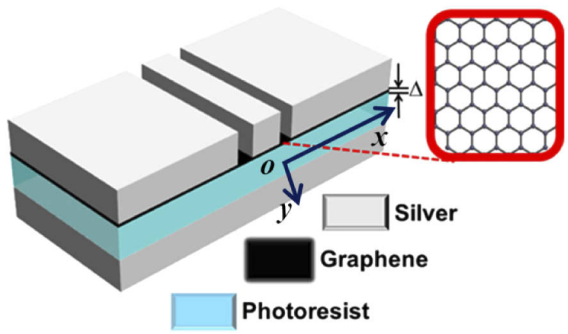

Fig. 1. Schematic of the graphene based simple double slits superlens. The slits are milled on the surface silver film, the graphene and photoresist layers are sandwiched in the silver slabs.

In this work, the graphene layer is introduced as a 0.335nm thickness dispersive medium by using the optical conductivity formula that is derived within the random-phase approximation (PRA) in the local limit [20,21]:

$$\tilde{\sigma}_{\text{intra}} = \frac{2ie^2 k_B T}{\hbar^2 \pi(\omega + i{\tau_g}^{-1})} \ln\left[2\cosh\left(\frac{E_F}{2k_B T}\right)\right] \tag{1}$$

$$\widetilde{\sigma}_{\text{inter}} = \frac{e^2}{4\hbar}\left[\frac{1}{2} + \frac{1}{\pi}\arctan\left(\frac{\hbar\omega - 2E_F}{2k_B T}\right)\right] - \frac{e^2}{4\hbar}\left[\frac{i}{2\pi}\ln\frac{(\hbar\omega + 2E_F)^2}{(\hbar\omega - 2E_F)^2 + (2k_B T)^2}\right] \tag{2}$$

In the equation set, T is the temperature taken as 300K at room temperature, k_B is the Boltzmann constant and E_F is the Fermi energy of excited graphene. The scattering lifetime of electrons in excited graphene is given by

$$\tau_g = \frac{\mu E_F}{e{v_F}^2} \tag{3}$$

Where the impurity-limited dc conductivity $\mu \approx 10000\ \text{cm}^2/(\text{V}\cdot\text{s})$ and the graphene Fermi velocity $v_F = 10^6$ m/s [22,23]. As for the tunability of this excited graphene based superlens structure, changes of the Fermi energy would lead to a simultaneous change in the interband threshold and the interband transition owing to the unique linear dispersion relation of graphene [24]. However, as the Fermi energy is increased, some of the interband transitions are blocked

Optical Materials EXPRESS

and hence leads to a narrower resonance. As a result, Fermi energy modification leads to tunable surface optical conductivity, which includes the contributions from intraband transitions and interband transitions of excited graphene.

The excitation spectrum of normalized electric field (e-field) enhancement collected from one slit of the designed graphene-based superlens is shown in Fig. 2. The simulations are performed at wavelengths of visible spectrum from 560 nm to 660 nm. It should be noticed that the intrinsic graphene with Fermi energy 0.1 eV is taken here. It clearly shows that more than 235 times enhancement of the nomalized electric field can be observed in the designed superlens with spectral peak centered at 608 nm. It physically originates from the hybrid plasmon excitation of the graphene based slits-cavity structure, in which the graphene-silver hybridization resonance dominantly attributes to the enhanced electric field of the slits superlens. The graphene Fermi energy tuning of electric field amplitude is shown in inset of Fig. 2. We can see that the electric field amplitude amplification factor defined as |E/E0| can be further enhanced via increasing graphene Femi energy from -1.5 eV to 1.5 eV in theory. However, it can be experimentally realized by applying electrostatic gate doping depending on the voltage threshold [25]. We believe more powerful tunabilty for practical plasmonic enhancement application can be expected by applying few layer graphene(FLG) at higher DC biased voltage. Consequently, the strong enhancement of electric field in the superlens can be expected via optimizing the elements of graphene for the nanoslits superlens. The results can guide for designing the low-cost and simple-realized superlens, projecting the interference image of the large electric field intensity.

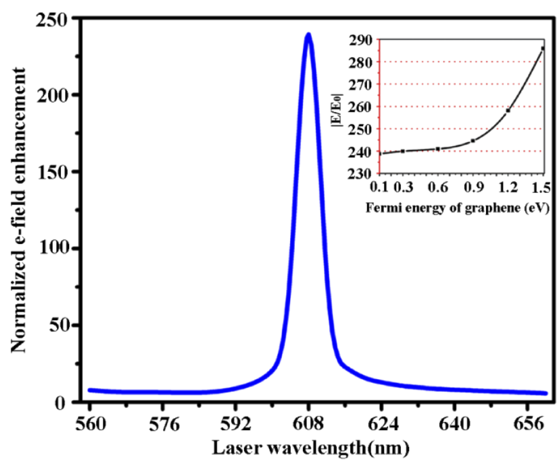

Fig. 2. The excitation spectrum of normalized electric field enhancement collected from one slit of the designed graphene-based sandwich superlens. The slit width is set as 10nm and the index of refractive of photoresist is 1.59. The silver film slab with thickness of 40 nm.

The electric field amplification properties for plasmonic interference imaging recorded in photoresist, including the amplitude amplification factor (a) and the electric field profile(b) with respect to slit width of the designed superlens in cases with and without graphene layer are shown in Fig. 3. Here, the enhanced electric field profile is defined as E/E_0, where E denotes the localized electric field, E_0 means the incident electric field of laser, treated as unit 1 here. The index of reflective for photoresist is set as 1.59. We can see from Fig. 3(a) that the electric field amplitude amplification factor can be significantly increased in case with graphene layer especially as the slit width is reduced to 10 nm. It indicates the amplification factor can be further enhanced as a narrower slot is selected in designing the superlens. A more than 4 times enhancement of the electric field amplitude is observed for graphene-based surplens with 10 nm

Optical Materials EXPRESS

slit compared to that without graphene layer. When the slit width increases to be larger than 40 nm, the amplification factor can be continuously impaired until it nearly approaches zero in both cases with and without graphene. In fact, the plasmonic cavity interference assisted by the two slits plays a key role in forming the periodically spatial modulation of electric field. One of the segmented hybrid plasmonic mode as the periodic electric field distribution is shown in inset of Fig. 3(a). For comparison, the enhanced electric field profiles for the superlens with the typical slit widths of 10 nm and 30 nm are calculated as shown in Fig. 3(b). For 10 nm slit width simulation, the graphene layer is used for the superlens. It can be clearly observed that the contrast of electric field profile in photoresist is significantly improved for 10 nm slit compared to 30 nm slit without graphene. More interestingly, the electric field profile peak recorded in photoresist layer for graphene based superlens shifts steadily towards two sides in x direction compared that without graphene. This originates from the modified surface plasmon waves assisted by the graphene plasmon, in which the accumulated charges support for short wave surface plasmon in regions near the graphene boundaries. The results are basically useful for understanding the interference image distribution of electric field for advanced plasmonic photolithography applications by designing the graphene based superlens.

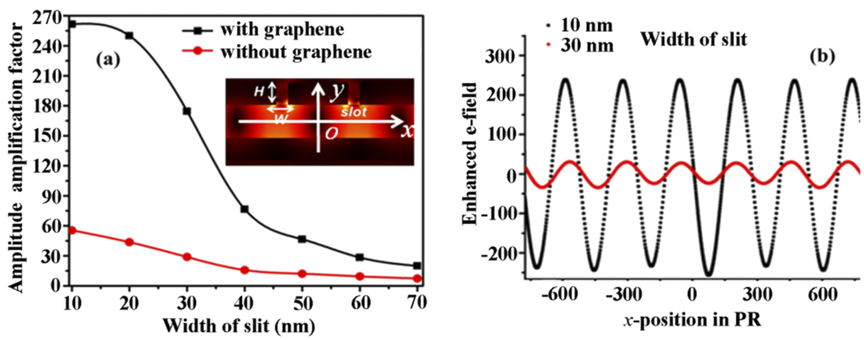

Fig. 3. The enhanced electric field properties for plasmonic interference imaging recorded in photoresist with respect to slit width of superlens in cases with and without graphene layer. The gold or silver slab layers are selected at the thickness of 40nm.

For advancing plasmonic photolithography imaging of the graphene-based superlens, careful selection of proper photoresist layer can be very important for improving imaging replica ability. Using the amplification effect of superlens on evanescent wave, the surface plasmon interference pattern can be imaged and then is exposed on photoresist, in which the refractive index and photoresist thickness all play important roles in affecting the photolithography performance of superlens. Figure 4 shows the simulated amplitude amplification factor for enhanced electric field of the plasmonic imaging in photoresist (PR) layer as a function of refractive index of photoresist at the designed wavelength of 608 nm. The PR thickness is taken as 60 nm in the simulation. We can clearly see that the amplitude amplification factor slightly increases as the refractive index of photoresist increases from 1.5 to 1.56. However, it exhibits a rapid rise when the refractive index of photoresist gets to be larger than 1.56. In fact, the plasmonic interference image can be recorded in photoresist or not, depending on the enhanced electric field profile in general photoresist medium. We believe the alternative recording layer with higher index of refractive like TiO_2, HfO_2 can also potentially function as high-quality plasmonic imaging medium with low energy loss due to the small extinction coefficient [26,27]. The higher index of refractive for recording medium of TiO_2, HfO_2 can be potentially helpful for enhancing the electric-field amplification factor. However, the pattern transfer process using TiO_2 or HfO_2 as the meduim is still an open question and so far compared to well-known photoresist medium. Therefore, some complex engineering trial is still needed to define the feasibility for using TiO_2 or HfO_2 instead

Optical Materials EXPRESS

of conventional photoresist for the plasmonic imaging. The spatial electric field distribution (profile) for different PR refractive index is shown in insert of Fig. 4. It indicates that the highly enhanced electric field profile for the superlens can be assured as considering the photoresist with higher refractive index of 1.6. The results can be potentially helpful for designing the superlens via properly selecting refractive index of photoresist for advancing plasmonic photolithography.

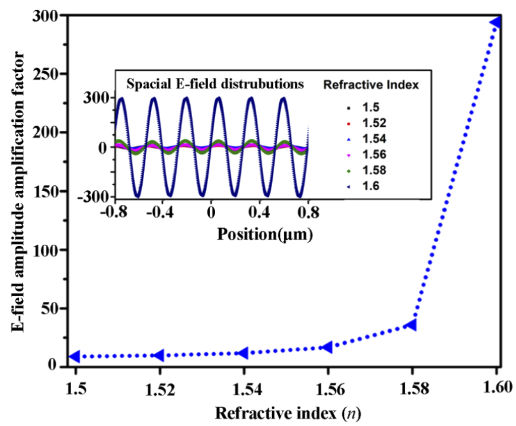

Fig. 4. The simulated electric field amplitude amplification factor for plasmonic imaging in photoresist (PR) layer as a function of refractive index of photoresist. The gold or silver slab layers are selected at the thickness of 40nm and the slits width is considered as 10nm.

The enhanced electric field profiles for the designed graphene based superlens with respect to different thicknesses of photoresist is shown in Fig. 5. It can be seen that the electric field profile enhancement clearly appears in photoresist medium for the photoresist thickness of 60 nm as in Fig. 5(a). On the contrary, 40 nm thickness photoresist results in almost disappearing of the electric field profile. Here, the index of refractive for photoresist is set as 1.6, the slits width is considered as 10 nm. In order to well design the superlens for amplified plasmonic nano-imaging with high-fidelity, we further simulate the electric field amplitude amplification factor for the plasmonic interference imaging as a function of the photoresist thickness as shown in Fig. 5(b). It clearly indicates that the amplitude amplification factor thoroughly attenuates as the photoresist thickness deviates from the optimal one of 60 nm. Also, we find that using the graphene based superlens can be greatly beneficial for highly enhanced electric field imaging, but has nothing to do with selecting optimal thickness of photoresist in the current design. The results can be explained as surface plasmon resonance tuned by surperlens cavity medium, which is physically satisfied for the 60 nm photoresist in superlensing. However, as the photoresist thickness slightly deviates from 60 nm, the surface plasmon resonance gets weakened and even invalid, indicating the importance of selecting the photoresist for advanced plasmonic photolithography. We believe the active plasmonic tunability can be the futher solution route for plasmonics imaging performance improvement. The active plasmonics via external thermal, optical or electric sources can be great promising for the plasmonics imaging applications. Especially, the temperature-dependent tunability of the optical contrast can be exhibit great prospect for the active plasmonics applications [28].The photo-lithography imaging quality improvement can be highly expected via actively manipulating the new elements of PCMs in near future.

The enhanced electric field profiles in photoresist layer for the designed superlens with respect to different slab layers of gold and silver is shown in Fig. 6. Here, the gold or silver slab layers are selected at the thickness of 40 nm and the slits width is considered as 10 nm. We can see from (a) that the electric field profile is significantly enhanced for the silver film slab compared

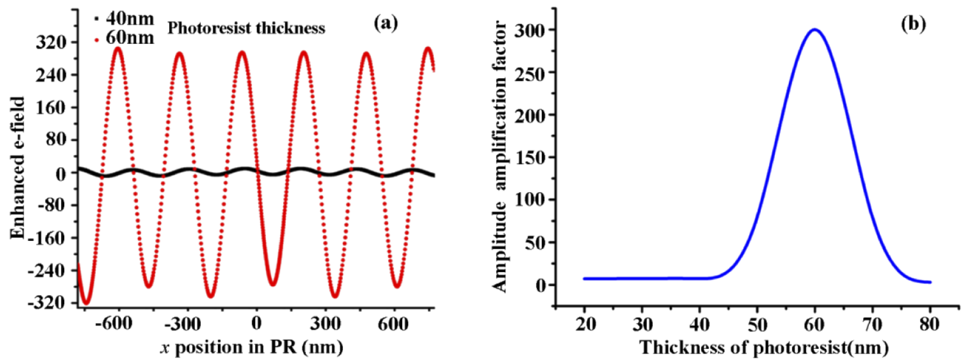

Fig. 5. The enhanced electric field profiles for the designed graphene based superlens with respect to thickness of photoresist. The gold or silver slab layers are selected at the thickness of 40nm.

to the gold one at working wavelength 608 nm. As the silver film slab is utilized, the electric field profile contrast of interference image is very poor. In this case, the superlens can not well function for imaging in the photoresist layer. In order to understand the unique role of silver slab layer, we carry out the comparable simulations on the enhanced electric field profile in cases with and without silver slab layer as seen in Fig. 6(b). It is obviously seen that as the silver slab is included in the superlens, the strong electric field profile for forming the clear interference imaging can be definitely recorded in the photoresist layer. Once the silver slab is removed, the characteristic electric field interference profile disappears. It originates from the Fabry-Perot like cavity geometry, in which the Ag-Graphene-Ag hybridization plasmon can be qualified for generating strong plasmon resonance, supporting the strong enhanced electric field. The low loss cavity design can be greatly helpful for reducing the total damping rate as Ag is placed very close to graphene. As a result, the visible hybrid mode is observed from the Ag-Graphene-Ag cavity system due to enhanced interband transition for the low loss graphene-based cavity geometry. The results are helpful for optimizing the superlens padding layer structures for forming the high-contrast patterns for high-quality superlens plasmonic imaging for advanced photolithography related applications.

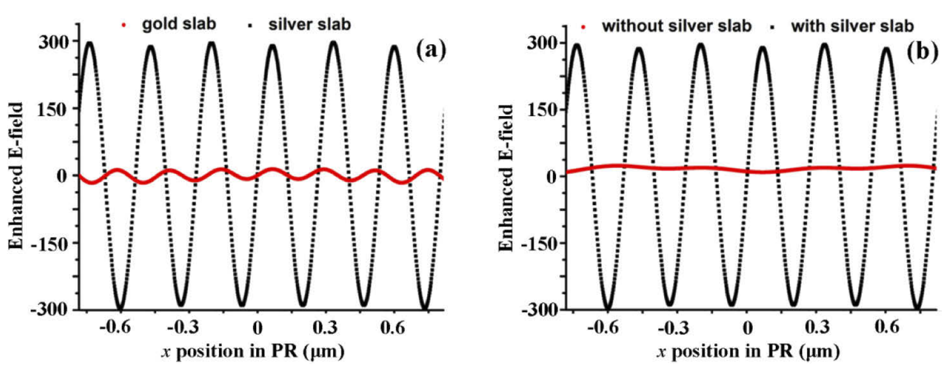

Fig. 6. The enhanced electric field profiles in photoresist for the designed superlens with gold and silver slab, respectively (a), and taking into account silver slab and without silver slab (b). The gold or silver slab layers are selected at the thickness of 40nm.

Optical Materials EXPRESS

3. Conclusions

In summary, we have theoretically investigated graphene participating in improving the interference imaging pattern quality via designing graphene based simple double-slits superlens. It is revealed that more than 235 times electric field enhancement is definitely assured by introducing graphene in the optical plamonic superlens. It shows the electric field amplitude amplification factor can be significantly increased in case with graphene layer. More than 4 times enhancement of electric field amplitude is observed for optimal slit structures of graphene-based surplens compared to that without graphene layer. It clearly indicates that the amplitude amplification factor attenuates as the photoresist thickness deviates from optimal one of 60 nm. The results are attributed to the unique role of graphene participating in hybrid plasmonic cavity modes modulating of the localized electric field from nanoslits of superlensing. This study shows that proper designing of graphene-based hybrid superlens can realize gaint enhancement of interference patterning for high-quality optical imaging of superlens.

Funding

National Key Research and Development Program of China (2017YFB1104700); National Natural Science Foundation of China (61875158, 61775177); Shaanxi Province National Science Foundation (2019JM-070); International Joint Laboratory for MicroNano Manufacturing and Measurement Technologies; Fundamental Research Funds for the Central Universities.

Disclosures

The authors declare no conflicts of interest.

References

1. X. Zhang and Z. Liu, "Superlenses to overcome the diffraction limit," Nat. Mater. **7**(6), 435–441 (2008).
2. J. Dong, J. Liu, X. Zhao, P. Liu, J. Liu, G. Kang, J. Xie, and Y. Wang, "A super lens system for demagnification imaging beyond the diffraction limit," Plasmonics **8**(4), 1543–1550 (2013).
3. Z. Zhao, Y. Luo, W. Zhang, C. Wang, P. Gao, Y. Wang, M. Pu, N. Yao, C. Zhao, and X. Luo, "Going far beyond the near-field diffraction limit via plasmonic cavity lens with high spatial frequency spectrum off-axis illumination," Sci. Rep. **5**(1), 15320 (2015).
4. H. Li, L. Fu, K. Frenner, and W. Osten, "Cascaded plasmonic superlens for far-field imaging with magnification at visible wavelength," Opt. Express **26**(8), 10888–10897 (2018).
5. D. Lu and Z. Liu, "Hyperlenses and metalenses for far-field super-resolution imaging," Nat. Commun. **3**(1), 1205 (2012).
6. H. Liu, B. Wang, L. Ke, J. Deng, C. C. Chum, S. L. Teo, L. Shen, S. A. Maier, and J. Teng, "High aspect subdiffraction-limit photolithography via a silver superlens," Nano Lett. **12**(3), 1549–1554 (2012).
7. L. Fang, L. Pan, C. Wang, and X. Luo, "Superlens imaging lithography for high aspect ratio sub-wavelength pattern employing trilayer resist process," Microelectron. Eng. **110**, 35–39 (2013).
8. T. M. Hien and H. T. Dung, "Image of an emitting dipole by a superlens," Phys. Rev. A **85**(1), 015804 (2012).
9. A. O. Bak, V. Giannini, S. A. Maier, and C. C. Phillips, "Super-resolution with a positive epsilon multi-quantum-well super-lens," Appl. Phys. Lett. **103**(26), 261110 (2013).
10. F. Wang, L. Liu, H. Yu, Y. Wen, P. Yu, Z. Liu, Y. Wang, and W. J. Li, "Scanning superlens microscopy for non-invasive large field-of-view visible light nanoscale imaging," Nat. Commun. **7**(1), 13748 (2016).
11. D. Chahinez, T. Reji, and R. Andreas, "Modeling of the surface plasmon resonance tunability of silver/gold core–shell nanostructures," RSC Adv. **8**(35), 19616–19626 (2018).
12. A. Lombardi, M. P. Grzelczak, A. Crut, P. Maioli, I. Pastoriza-Santos, L. M. Liz-Marzán, N. D. Fatti, and F. Vallée, "Optical response of individual Au-Ag@SiO2 heterodimers," ACS Nano **7**(3), 2522–2531 (2013).
13. J. Dong, J. Liu, G. Kang, J. Xie, and Y. Wang, "Pushing the resolution of photolithography down to 15nm by surface plasmon interference," Sci. Rep. **4**(1), 5618 (2015).
14. G. Liang, C. Wang, Z. Zhao, Y. Wang, N. Yao, P. Gao, Y. Luo, G. Gao, Q. Zhao, and X. Luo, "Squeezing Bulk Plasmon Polaritons through Hyperbolic Metamaterials for Large Area Deep Subwavelength Interference Lithography," Adv. Opt. Mater. **3**(9), 1248–1256 (2015).
15. X. Yang, B. Zeng, C. Wang, and X. Luo, "Breaking the feature sizes down to sub-22 nm by plasmonic interference lithography using dielectric-metal multilayer," Opt. Express **17**(24), 21560–21565 (2009).

Optical Materials EXPRESS

16. W. Adams, A. Ghoshroy, and DÖ Güney, "Plasmonic superlens image reconstruction using intensity data and equivalence to structured light illumination for compensation of losses," J. Opt. Soc. Am. B **34**(10), 2161–2168 (2017).
17. C. Jeppesen, R. B. Nielsen, A. Boltasseva, S. Xiao, N. A. Mortensen, and A. Kristensen, "Thin film Ag superlens towards lab-on-a-chip integration," Opt. Express **17**(25), 22543–22552 (2009).
18. F. Javier and G. de Abajo, "Graphene plasmonics: Challenges and opportunities," ACS Photonics **1**(3), 135–152 (2014).
19. P. Nene, J. H. Strait, W. M. Chan, C. Manolatou, S. Tiwari, P. L. McEuen, and F. Rana, "Coupling of plasmon modes in graphene microstructures," Appl. Phys. Lett. **105**(14), 143108 (2014).
20. L. A. Falkovsky and A. A. Varlamov, "Space-time dispersion of graphene conductivity," Eur. Phys. J. B **56**(4), 281–284 (2007).
21. L. A. Falkovsky and C. C. Pershoguba, "Optical far-infrared properties of graphene monolayer and multilayers," Phys. Rev. B **76**(15), 153410 (2007).
22. K. S. Novoselov, A. K. Geim, S. V. Morozov, D. Jiang, Y. Zhang, S. V. Dubonos, I. V. Grigorieva, and A. A. Firsov, "Electric field effect in atomically thin carbon films," Science **306**(5696), 666–669 (2004).
23. J. Christensen, A. Manjavacas, S. Thongrattanasiri, F. H. L. Koppens, and F. J. G. de Abajo, "Graphene plasmon waveguiding and hybridization in individual and paired nanoribbons," ACS Nano **6**(1), 431–440 (2012).
24. T. Low and P. Avouris, "Graphene plasmonics for terahertz to mid-infrared applications," ACS Nano **8**(2), 1086–1101 (2014).
25. Y. Zhang, Y. Feng, B. Zhu, J. Zhao, and T. Jiang, "Graphene based tunable metamaterial absorber and polarization modulation in terahertz frequency," Opt. Express **22**(19), 22743–22752 (2014).
26. W. T. Chen, A. Y. Zhu, V. Sanjeev, M. Khorasaninejad, Z. J. Shi, E. Lee, and F. Capasso, "A broadband achromatic metalens for focusing and imaging in the visible," Nat. Nanotechnol. **13**(3), 220–226 (2018).
27. O. Hemmatyar, S. Abdollahramezani, Y. Kiarashinejad, M. Zandehshahvar, and A. Adibi, "Full color generation with Fano-type resonant HfO2 nanopillars designed by a deep-learning approach," Nanoscale **11**(44), 21266–21274 (2019).
28. S. Abdollahramezani, O. Hemmatyar, H. Taghinejad, A. Krasnok, Y. Kiarashinejad, M. Zandehshahvar, A. Alù, and A. Adibi, "Tunable nanophotonics enabled by chalcogenide phase-change materials," Nanophotonics **9**(5), 1189–1241 (2020).